Supplementary Material Available: The final atomic coordinates of Cu₄MgPh₆·Et₂O (Table A) and [Cu₄LiPh₆]⁻[Li(Et₂O)₄]⁺·2Et₂O (Table B) (2 pages). Ordering information is given on any current masthead page.

Thermochromic Transformations of 2,6-Diorgano-1,3,5,7-tetraoxa-2,6-dibora-4,8-octalindiones: A Model for Solid-State Phase Transformations and Hysteresis

Mohamed Yalpani,* Walter R. Scheidt, and Klaus Seevogel

Contribution from the Max-Planck-Institut für Kohlenforschung, Kaiser-Wilhelm-Platz 1, D-4330 Mülheim an der Ruhr, West Germany. Received June 8, 1984

Abstract: The mechanisms underlying phase transformations and hysteresis have been investigated by using the example of the phase changes resulting from the solid-state thermochromic reactions of **1a–i**. It is found that the transition "order" is strictly dependent on the morphology of the solids used. Thus, polycrystalline samples of **1** give diffuse transitions, while with tempered and almost homogeneous crystals, nearly isothermal transitions are obtained. Pressure thermograms and substituent effects point to a generalized model for hysteresis phenomena which suggests an interdependence of the ΔH of the chemical reaction and of the ensuing lattice or conformational changes in a transforming system.

We recently described the preparation,[1] the X-ray structure analysis, and the mechanism[2] of the solid-state polymerization–depolymerization and thermochromic reaction of the boraheterocycle **1**. The cell dimensions of the single crystal of **1b**, de-

	R
1a	CH₃
b	C₂H₅
c	n-C₃H₇
d	i-C₃H₇
e	i-C₄H₉
f	c-C₆H₁₁
g	n-C₈H₁₇
h	n-C₁₆H₃₃
i	CH₂C₆H₅
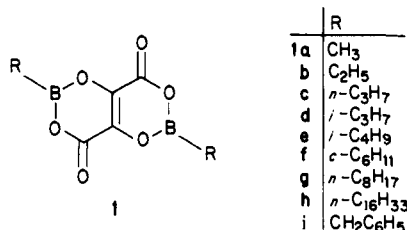
termined between −73 and +40 °C, indicated considerable volume changes.[2] It could thus be expected that this reaction is accompanied by one or more phase changes. Furthermore we had observed a very significant hysteresis in the thermochromic temperature T_{th}. In view of the paucity of reports on fully reversible solid-state organic reactions (cf. recent reviews on organic solid-state reactions[3]), and the continued interest in this still not fully understood field of chemistry, we set out to extend our investigations on this reaction. In particular we hoped to gain insights into the mechanism of the unusually large hysteresis effects observed for the various derivatives of **1**.

Results

Thermal Rearrangement of 1 under a Kofler Hot-Stage Microscope. Preliminary observations of the crude crystals of **1c**, as separated from the reaction mixture, under a hot-stage microscope showed them to be thin yellow plates, some of which were hexagons of uniform size. Heating them at a rate of about 1 °C/min through the T_{th} at about +75 °C resulted in a uniform color change (yellow to colorless) within about 0.5 °C. When cooled the thermochromic change (colorless to yellow) set in at about +55 °C and was completed within 0.5 °C. In the heating

and cooling cycles, no visual change of the crystal dimensions could be detected. Neither could any cracking or shattering of the crystals be observed. Also the colored (colorless) areas formed showed the same extinction direction between crossed polarized light as did the starting crystals. Sublimation of the above crude crystals gave mostly a polycrystalline mass. Under the microscope they appeared layered and twinned, and nearly all were of undefined shape. The transition of the individual polycrystals through T_{th} was no longer uniform. Color change commenced successively at different points in each layer of the polycrystals and moved across the layers as a "liquid" front (compare Figure 2 in ref 4). This process was completed within about 2 °C. When the heating and cooling cycles were retraced, the same starting points for the color change were observed in any one polycrystal.

DSC Analysis of 1. Figure 1 shows heating and cooling scans for crude crystals of **1b** and **c**, respectively. The effect of sublimation on the heating scans of **1c** is shown in Figure 2. In Figure 3 is shown that the onset temperature for the change is, over a wide range, nearly independent of the heating rate. The variations of the peak transition temperature (T_p) with applied mechanical pressure on solid **1c** and **b** are shown in Figures 4 and 5, respectively. A summary of selected results of the DSC measurements for the various derivatives of **1** is given in Table I.

Infrared Studies. Figure 6A and B shows the infrared spectra in the region of 2000–400 cm⁻¹ of the high- and low-temperature forms of **1c** taken at +95 and −20 °C, respectively. Prominent among the changes are the peaks in the region between 1950 and 1500 cm⁻¹. The two peaks at 1760 and 1735 cm⁻¹ of the "hot" form can be assigned to free carbonyl stretchings. In the "cold" form, these have decreased drastically and have become replaced by two bands at 1645 and 1550 cm⁻¹ assignable to chelated carbonyl stretchings. Figure 6C shows the effect of sublimation on the infrared spectrum of **1c**. In Figure 7A the integrated intensities of the peaks at 1760 and 1735 cm⁻¹ of sublimed crystals of **1c** through three heating and cooling cycles are plotted against temperature. This figure also clearly shows the pronounced hysteresis in the heating and cooling process. The effect of in-

(1) Yalpani, M.; Köster, R. *Chem. Ber.* **1983**, *116*, 3332.
(2) Yalpani, M.; Boese, R.; Bläser, D. *Chem. Ber.* **1983**, *116*, 3338.
(3) Paul, I. C.; Curtin, D. Y. *Acc. Chem. Res.* **1973**, *6*, 217. Gavezzotti, A.; Simonetta, M. *Chem. Rev.* **1982**, *82*, 1.

(4) McCullough, D. Y., Jr.; Curtin D. Y.; Paul, I. C. *J. Am. Chem. Soc.* **1972**, *94*, 874.
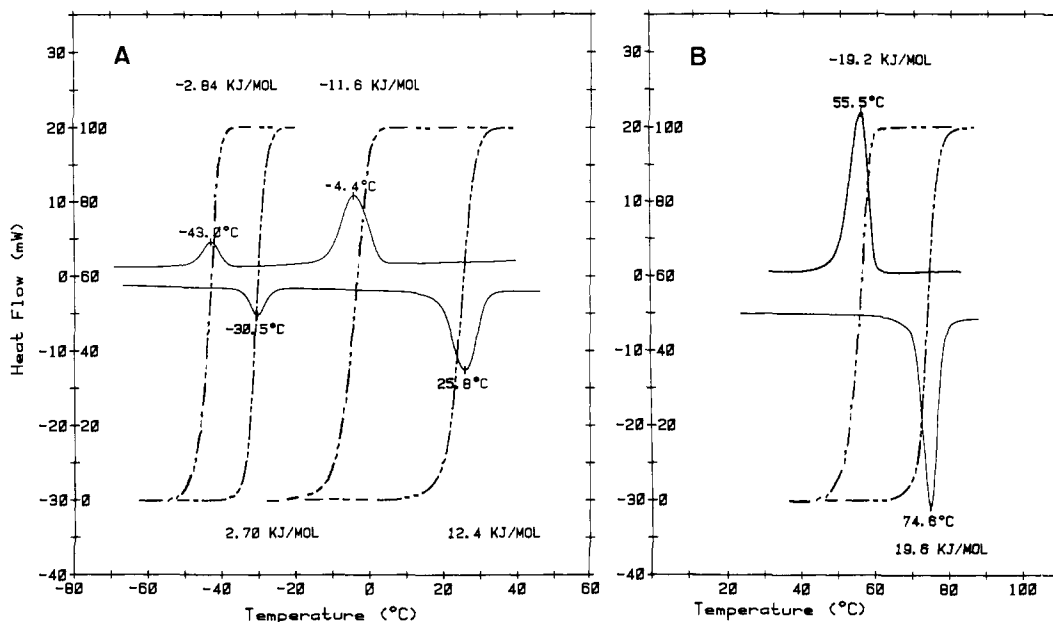
Figure 1. DSC heating and cooling scans for crude crystals of **1b** and **c**.
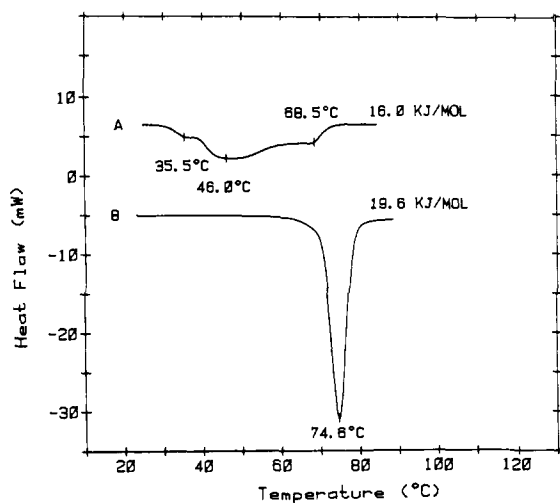

Figure 2. Effect of sublimation on the DSC heating scans of (A) sublimed crystals compared with that of (B) crude crystals of **1c**.

terrupting the heating process at some points during the phase transformation followed by reversing the cycle on the shape of

the hysteresis loops (scanning curves) is shown in Figure 7B. Repeated heating and cooling cycles and hysteresis loops of a sample of **1c** aged at room temperature for about $1^1/_2$ years is shown in Figure 8. This figure also shows the full reversibility of the polymerization–depolymerization reaction.

Equilibration Attempts. Two samples of **1c**, one in the colorless "hot" and the other in the yellow cold form, were both inserted into a temperature bath maintained at about +65° and kept for 1 week. Both samples retained their original colors. This experiment was repeated with the colorless and yellow forms of **1b** at +8 °C. As in the previous experiment, both samples retained their original colors.

Discussion

Transition "Order". From preliminary observations of the behavior of the various batches of crystals of **1** under the hot-stage microscope, it was clear that for the planned thermal and infrared spectroscopic studies the crystal morphology and history would define the results. In agreement with this, it can be seen by comparing Figures 2, 7, and 8 that upon "purification" by sublimation, the onset temperature for crystals of **1c** is lowered and causes the process to take place over a broader range. It thus appears that the crystalline mass obtained by sublimation, even though chemically purified, becomes crystallographically inhomogeneous.
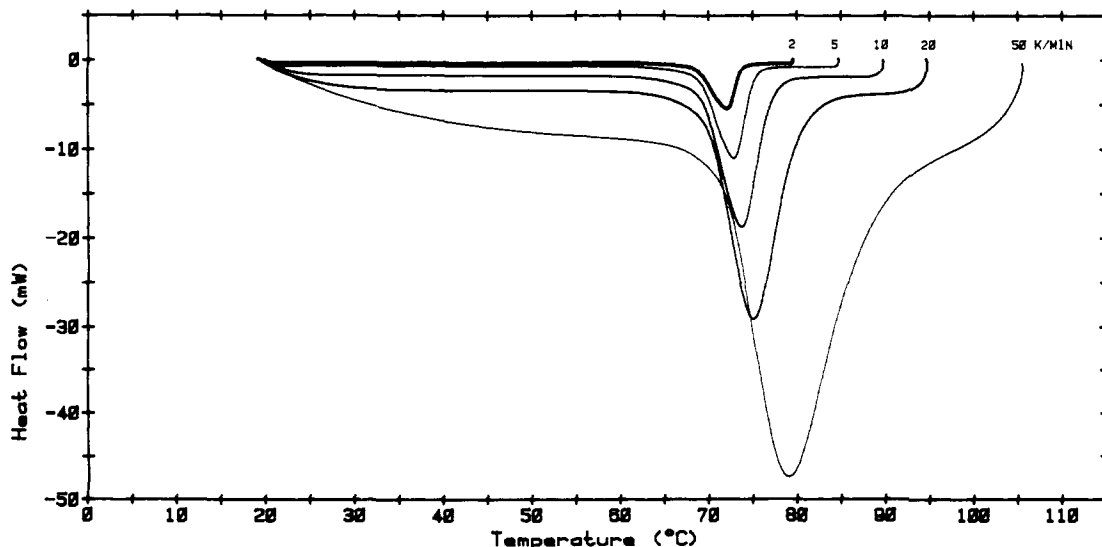

Figure 3. Effect of increasing the scanning rate on the onset temperature for the transition of aged crystals of **1c** to the "hot" form.

Table I. Thermal Transition Parameters for Substituted **1**

1	range of measurement, °C	heating		cooling		hysteresis	
		$T_{y \to c}$,[a] °C	T_p, °C	$T_{c \to y}$, °C	T_p, °C	ΔT_p	ΔH, J/g
a, CH_3	−70 to + 120	∼25	25	∼ −5[b]		∼30	c
b, C_2H_5[d]	−70 to +60	17	−30.5/+26	+5	−4/−43	30	55.4[d]
c, $n\text{-}C_3H_7$	−70 to +100	75	75	55	55	18	78.6
d, $i\text{-}C_3H_7$	rt[g] to +165	150	150	106	103	47	112.0
e, $i\text{-}C_4H_9$	rt to +115	72	84	48	43	41	56.1
f, $c\text{-}C_6H_{11}$	rt to +115	88	91	49	44	47	67.0
g, $n\text{-}C_8H_{17}$	rt to +110	75	70/90	55	81/50	20	56.0[e]
h, $n\text{-}C_{16}H_{33}$	rt to +125	11	118	85	81	37	
i, $CH_2C_6H_5$	rt to +125	87/98[f]	93	60/45	62	31	33.5[e]

[a] y = yellow; c = colorless. [b] Determined visually, no cooling run. [c] DTA runs only. [d] ΔH for the thermochromic transition only. [e] ΔH for sum of both transitions. [f] Color changes from orange to yellow to colorless. [g] Room temperature.
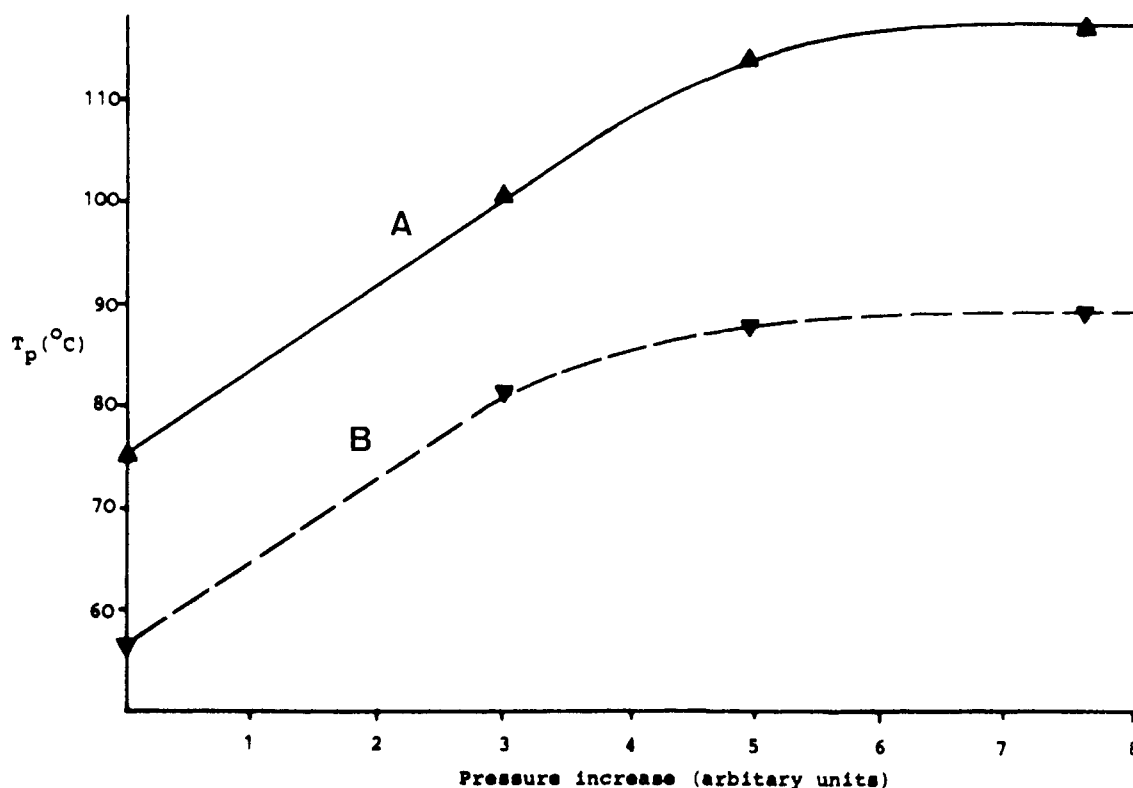
Figure 4. Effect of pressure on the transition temperature (T_p) and hysteresis of **1c**: (▲) heating, (▼) cooling scans.
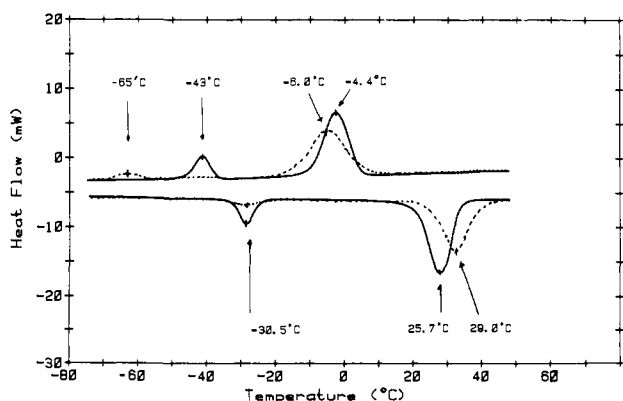
Figure 5. DSC curves showing the phase changes of **1b** at ambient (—) and under mechanical pressure (...).

Residual disorder and strain present in the crude crystals of **1c** appear to decrease further when crude crystals of **1c** are left standing at room temperature for more than 1 year. This can be clearly seen from comparison of the shape of the thermal transition curve of a sample freshly prepared (Figure 7B) with that of an aged one (Figure 8). The aged crystals show a more abrupt transition over a temperature range of less than 20 °C.

The greater part of this occurs in less than 10 °C. It would thus appear that the stored sample has undergone some degree of crystal modification or reforming. This could also be inferred from the visual appearance of the crystals. The aging had brought about a change of the color to yellow–orange from bright yellow, and under the microscope, a large portion of the crystals was hexagons of uniform size. A further indication of the importance of crystal homogeneity could also be obtained from the room temperature ("cold" modification) infrared spectrum of the aged crystals in which the two residual carbonyl bands at 1760 and 1735 cm⁻¹ (compare Figure 6B) have vanished. Conversely, when the aged crystals were sublimed and the sublimate collected on a cold finger cooled to −40 °C, it showed both the low- and the high-temperature modifications of **1c** as indicated in its room-temperature infrared spectrum (Figure 6C).[5] The decrease of the enthalpy

(5) Sublimates of **1c** collected at about −180 °C were initially nearly colorless. When it was warmed to room temperature, the color changed to pale yellow, and the infrared spectrum obtained immediately after the sublimation showed the presence of the hot modification as the major component. This sample when left at room temperature overnight became more intense yellow and gave a modified infrared spectrum in which the cold modification was in slight excess. Nearly amorphous samples of **1b** were obtained when dihydroxyfumaric acid was stirred for 48 h at room temperature with an excess of triethylboroxine, and the volatiles were removed at high vacuum and 50 °C. This product, although chemically and spectroscopically (IR and MS) identical with crystalline **1b**, normally used in this study was only very weakly thermochromic when cooled down to −78 °C.
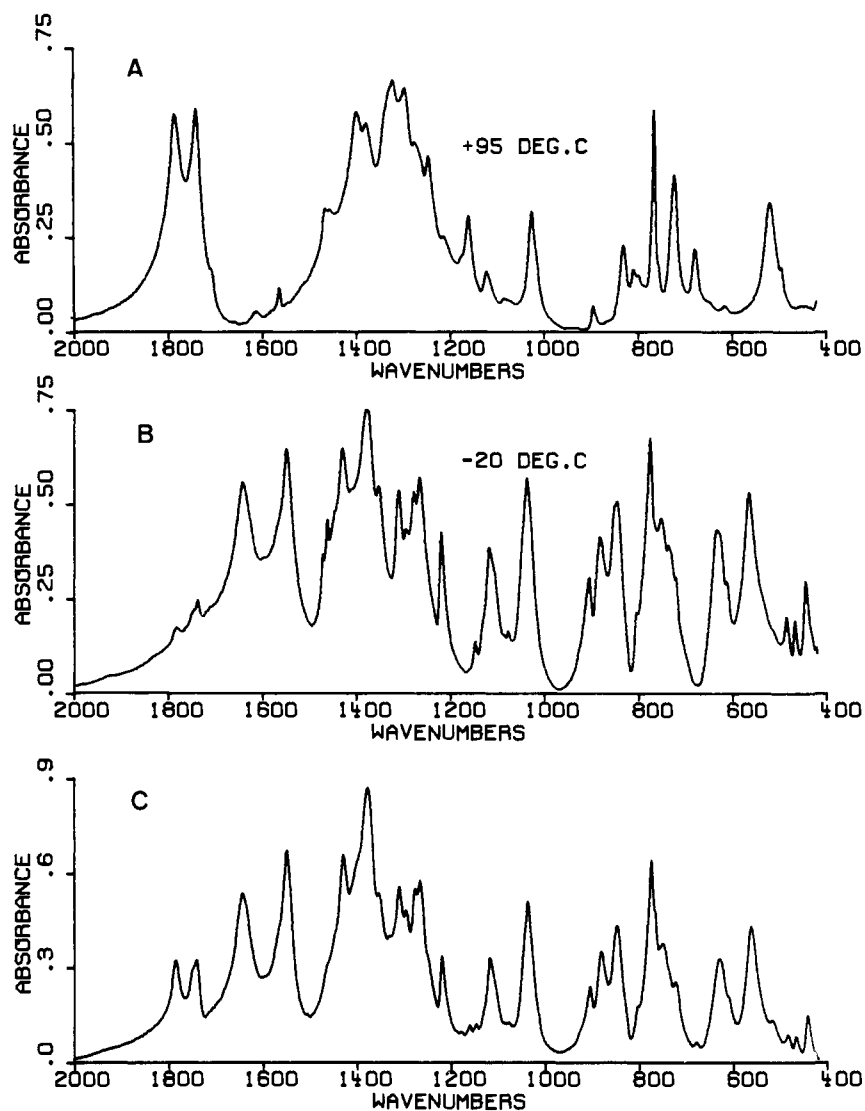
Figure 6. Infrared spectra (base-line corrected) of crude crystals of **1c** taken at (A) +95 °C, (B) -20 °C, and (C) of sublimed **1c** at room temperature.
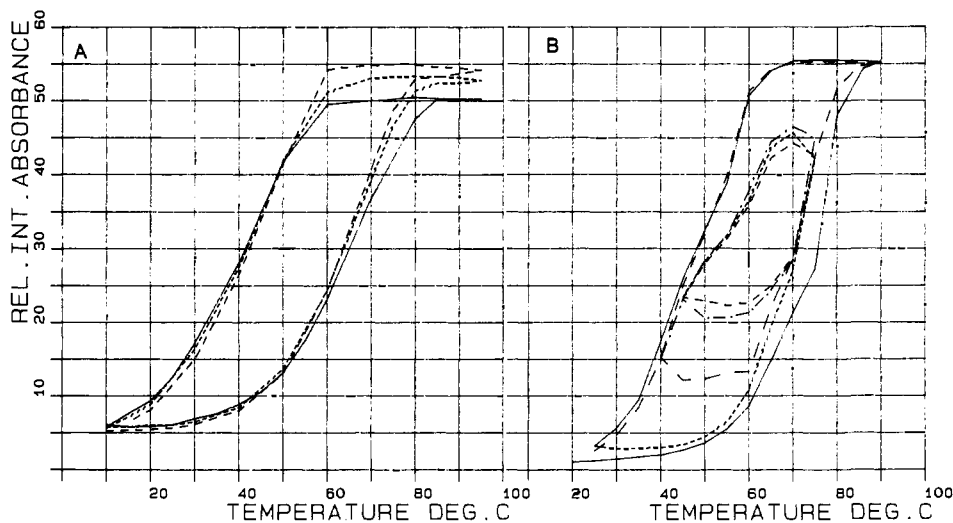

Figure 7. (A) Hysteresis loops of sublimed crystals of **1c** through three heating and cooling cycles: (—) cycle 1, (- - -) cycle 2, (- -) cycle 3 (relative integrated intensities are those of the carbonyl bands at 1760 and 1735 cm^{-1}). (B) Hysteresis loops and continuous scanning curves of crude crystals of **1c** through five heating and cooling cycles: (—) cycle 1, (- - -) cycle 2, ($\div$ -) cycle 3, (-·-) cycle 4, and (— —) cycle 5) (relative integrated intensities are those of the carbonyl bands at 1760 and 1735 cm^{-1}).

change for the transition (cf. Figure 2) by about 20%, as a result of sublimation, shows that only a smaller fraction of the molecules becomes totally disordered. The remainder are probably well ordered in crystallite pockets but due to the intrafacial forces

between the fused crystallites experience, varying degrees of hindrance to change. Furthermore, the overall lowering of the transition temperature shows that in the smaller crystallites, the transition barriers are reduced.[6]
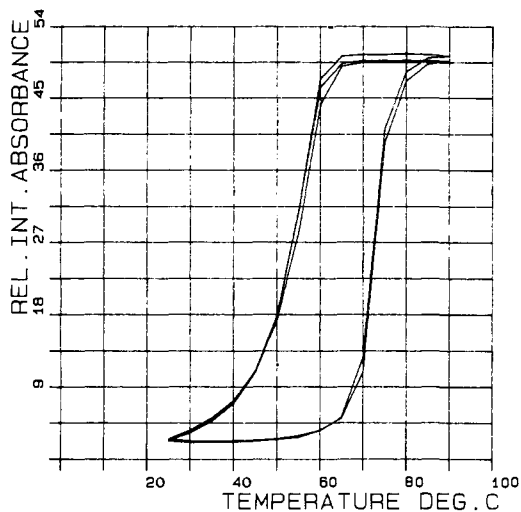
Figure 8. Hysteresis loops of aged crystals of **1c** through three heating and cooling cycles (relative integrated intensities are those of the carbonyl bands at 1760 and 1735 cm^{-1}).

These changes in the transition behavior resulting from differences in crystallinity, largely polycrystalline (sublimed crystals), microcrystalline to hexagons (crude crystals), and largely hexagons (aged crystals), point to the importance of crystal homogeneity for phase transformation studies. The various discussions[7] on the "order" (simple 1st, anomalous 1st, diffuse, "lambda" (λ), 2nd, etc.) of a transformation find their importance in the particular crystal assembly that has been used in the respective studies. In the case at hand, we have shown that depending on the shape and history of the crystals used for our studies, curves resembling those of first order, diffuse 2nd, or higher order transitions can be obtained. It also appears that if in a crystal assembly excess internal stresses are removed (in this case by aging or tempering), the transitions will be approximately discontinuous (isothermal). From our observations during the structure determinations,[2] where the room-temperature diffraction pattern of **1b** was diffuse and sharp photographs were only obtained after cooling well below or heating well above the transition points, it can be inferred that even in a single crystal, the homogeneity necessary for the observation of a truly isothermal transition may not be present. The sharp color transitions observed under the microscope for the aged single crystals also indicates that when stresses are removed, the single crystal as a whole behaves as a single "domain" and the necessity of complex considerations[7] of nucleation and interboundary effects are eliminated.

Hysteresis. For reversible transformations, a large number of hysteresis phenomena have been described in the physical, chemical, and biochemical literature. Thus, hysteresis cycles are well-known in ferromagnetism, ferroelectricity, adsorption–desorption cycles, solid transformations, and conformational changes in lipids and other biopolymers. Basically the elementary processes underlying the hysteresis imply a metastable state and an abrupt transition which in a larger assembly of elements generally appear as broad. Beyond this statement, the phenomenological descriptions recorded for the order–order transition in the solid state appear ambiguous both in terms of many of the terminologies used as well as the theoretical approaches to formulate this process.[7]

Figure 9. Everett model:[8] (A) Magnetomechanic circuit; (B) electric current *i* as a function of temperature.

In the early literature on this subject two mechanical analogies have been described.[8,9] However, to our knowledge, they have not been applied and related to a practical example of a chemical reaction in the solid state. This in part may have been due to the lack of a truly reversible solid-state reaction for which the exact structures of both states have been resolved and the chemistry involved fully understood.[10] The solid-state reaction of **1** for which the structures of the two phases as well as the chemistry have been fully elucidated can now be compared to one of these models to arrive at a simplified picture of the forces involved in this process.

In this model[8] (Figure 9), the temperature-dependent curve of the bimetal (BM) is combined with the temperature insensitive attractive forces of the two magnets (M). It is clear that the combination of these, i.e., the constant magnetic force and the variable temperature together, will determine the "on–off" position of the circuit. The magnets aid the closing of the circuit and hinder its reopening. It can thus be expected that the width of the hysteresis loop will be directly proportional, on the one hand, to the magnetic strength and, on the other, to the coefficient of thermal expansion of the bimetal. At zero magnet strength, the hysteresis should vanish and the temperature at which the switch opens or closes should converge on *T*.

For the thermally induced phase transformations of molecular systems such as **1**, in analogy to the above mechanical model, two basically independent factors can be identified: (a) the magnitude of the enthalpy change in the system undergoing a reaction (in this case the formation, or breakage of the chelate bond between the carbonyl oxygens of one molecule of **1** and the boron atoms of the neighboring molecules. As this is potentially an equilibrium reaction, it should, similar to the bimetal in the mechanical model, be a continuous function of temperature) and (b) the rigid crystal lattice in a solid, which is normally largely unaffected by temperature, unless heated to its melting point (order–disorder transition). In the order–order transitions considered here, the free interplay of the temperature-dependent chemical forces described in (a) will be restricted by the lattice structure of the crystal. Such a system, if defect-free, can be regarded as a single chemical entity or "domain". When heated or cooled, the individual reacting molecules, or subunits of this domain, will be prevented by the overall structure of the crystal to assume a Boltzmann distribution of reacted and unreacted species. When heated or cooled beyond a distinct temperature, the system must pass onto a metastable situation. At the end of this, the potential to undergo the reaction has increased to a point sufficient to overcome the lattice energies and pass into phase II. In order–disorder transitions, this would be the melting or sublimation point. In order–order transitions, the subunits of the domain can all pass directly and in unison or possibly after a disordered phase to a new order (compare discussions in ref 3). On retracing the process

(6) It has been observed that in the absorption of hydrogen gas on palladium metal, the transition temperature is lowered as the crystal size is reduced. Everett, D. H.; Sermon, P. A. *Z. Phys. Chem.* **1979**, *114*, 109. They also report an increase of the desorption pressure and therefore a decrease of hysteresis with decreasing crystal size. Similar effects have also been observed for the thermal transformations of small and large crystals of ammonium chloride. Thomas, D. G., Staveley, L. A. K. *J. Chem. Soc.* **1951**, 1420.

(7) Mayer, J. R.; Streeter, S. F. *J. Chem. Phys.* **1939**, *7*, 1019. Thomas, D. G.; Staveley, L. A. K.; Cullis, A. F. *J. Chem. Soc.* **1952**, 1727. Enderby, J. A. *Trans. Faraday Soc.* **1955**, *51*, 835; **1956**, *52*, 106. Ubbelohde, A. R. *J. Chim. Phys.* **1966**, *63*, 33. Rao, C. N. R.; Rao, K. J. *Prog. Solid State Chem.* **1967**, *4*, 131. Everett, D. H. *Colston Pap.* **1978**, *20*, 192. Liebau, F. *Fortschr. Mineral.* **1983**, *61*, 29.
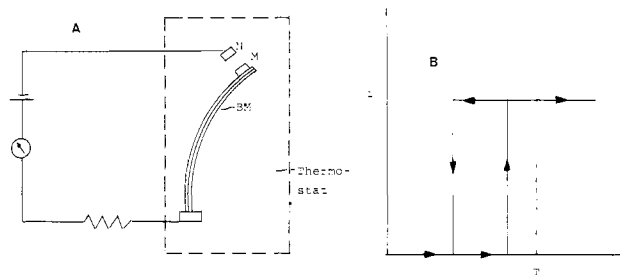
(8) Everett, D. H.; Whitton, W. I. *Trans. Faraday Soc.* **1952**, *48*, 749.

(9) Everett, D. H.; Smith, F. W. *Trans. Faraday Soc.* **1954**, *50*, 187.

(10) For the one, apparently, fully reversible solid-state reaction reported (Paul, I. C.; Go, C. K. T. *J. Chem. Soc. B* **1969**, 33) for which structures of the two phases have been determined, an analysis of the thermal transition has not been attempted. In other examples of reversible phase transformations, e.g. (Duesler, E. N.; Wiegers, J. E.; Curtin, D. Y.; Paul, I. C. *Mol. Cryst. Liq. Cryst.* **1980**, *59*, 289), it has not been conclusively established if in this single crystal $\rightleftharpoons$ single crystal interconversion, a solid-state reaction with molecular changes is also involved.
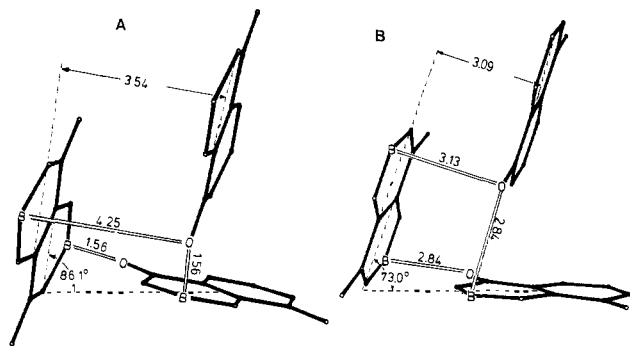
Figure 10. Contact distances and interplanar angles for molecules of **1b** in (A) "cold" and (B) the "hot" crystal modification.

in the opposite direction, hysteresis will arise if the lattice stabilities of the two phases do not coincide. In this case the reverse chemical change will again have to await the buildup of a potential sufficient to overcome the lattice forces of phase II. It is thus evident that the lattice forces act in a similar fashion in molecular systems as the magnets in the mechanical model. The results obtained and discussed below show several indicators which agree with the above picture.

(a) The effect of applied pressure on the T_p's for **1c** and **1b** are shown in Figures 4 and 5, respectively. It can be seen that as expected, the bond breakage reaction (upper curve Figure 4) becomes progressively more difficult (occurs at a higher temperature) as the pressure is increased. The rise of T_p with pressure is, however, not strictly proportional and levels out at higher applied pressures. For the cooling cycle (bond formation), a similar pressure effect can be observed. However, at higher pressures, the differences of T_p's (ΔT_p) for the heating and cooling cycles (width of hysteresis loop) are greater. To understand this effect, it is necessary to refer to the arrangement of molecules of **1** in the crystal lattice and the volume changes involved. Figure 10 shows the interrelation of three molecules of **1b** in the cold and hot forms, respectively.

It can be seen that while in the cold phase the nearly perpendicular molecules, as a result of chelate bond formation, have moved closer to each other, the parallel layers of molecules have a larger separation than in the hot phase. This results in a slightly smaller cell volume (523.6 Å^3 at 20 °C vs. 528.2 Å^3 at −30 °C)^2 in the hot phase. Furthermore, the interplanar angle decreases in going from the cold to the hot phase. It can be expected that as a result of pressure application, on the one hand, both of the volume and angle decreases would enhance the stability of the hot phase and, on the other, tend to prevent the breakage of the B–O bonds and their increased separation as required by the latter phase. The net results observed show that while the transition becomes hindered during the heating cycle and takes place at higher temperatures, once transformed it is relatively more stable (i.e., while the attractive forces between the reactive centers, C=O and B, remain relatively unaffected, the lattice energies of the two phases are affected differently by changes of pressure). This effect is also clearly evident in the case of pressure-dependent hysteresis of **1b** depicted in Figure 5. In this case, for the thermochromic transition, increase of pressure lowers the cooling T_p to below and elevates the heating T_p to above the observed at atmospheric pressure. Furthermore, it can be seen that the lower nonthermochromic transition has almost vanished.

(b) Another indication of the correctness of the analogy to the model described can be derived from the substituent effects on both ΔT_p as well as on T_p (Table I). Leaving out any lattice effects, it would be expected that as the electron-donating ability of the alkyl substituents increase in the order Me < Et < *i*-Pr, etc., the B–O chelate bond should be weakest for R = *i*-Pr and strongest for R = Me. The actual ΔT_p's and also the T_p's observed appear to be wholly unrelated to any such electronic effects. Without additional structural and lattice data on other substituted compounds (**1**), it is difficult to exactly identify the structural features responsible for the seemingly random values observed.
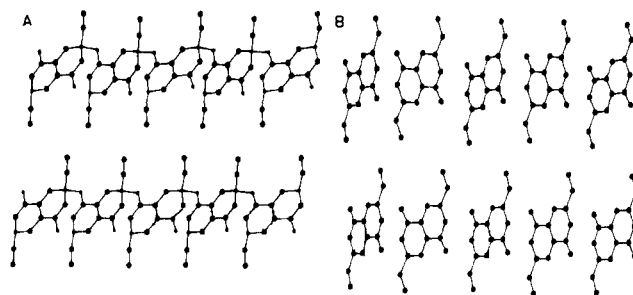

Figure 11. Arrangement of rows of molecules of **1b** in opposite stacks: (A) "cold" and (B) "hot" modification.

It can be assumed,^{11} however, that in all the derivatives of **1**, the basic solid-state structure is, if not identical, very similar to that found for **1b**. In these, the substituents in each stack of the molecules are oriented toward those in the next stack (see Figure 11) and at low temperature become intertwined. On warming from very low temperatures, initially the two stacks are pulled apart and the substituents become untangled. An indication for this process in **1b** is the low-energy transition observed at −43 °C (cooling) and −30.5 °C (heating), which coincides with the drastic expansion of the cell dimension along the *a* axis as the crystal was warmed from −73 to −30 °C.^{2} This process has probably no direct effect on the higher temperature thermochromic transition in consideration.^{12}

The lattice structural changes occurring at T_{th} are related to the movement of the molecules with respect to each other as the interplanar angle changes and also to the simultaneous movement of the substituents away from planarity with the hetero octaline ring as the boron atoms change their coordination from sp^2 to sp^3.

Due to the special arrangement of the stacks (cf. Figures 10 and 11), even if it is assumed that the above motions occur in concert and smoothly in any one stack, the substituents experience a steric hinderance as they pass, in an opposing direction, the substituents in the neighboring stacks. However, the differences in this steric hinderance exterted by the substituents should affect only the variations of T_p. As can be seen in Table I this is lower with the smaller substituents and increases roughly with the length of the alkyl chain and is more pronounced with branching. Nevertheless, from Table I it can be seen that chain length and branching have also an effect on ΔT_p. It is reasonable to assume that the substituents, due to their arrangement between the stacks, affect the relative static stabilities of the two phases differently and thereby cause changes in ΔT_p as well.

In general, when molecules in a lattice rearrange from one ordered form to another, and the change is caused by an internal chemical reaction, depending on the stability of phase I relative to phase II, the downhill chemical reaction may be aided or hindered. This then, by analogy to the mechanical model, results in the appearance of a hysteresis effect. The width of the loop, at a constant enthalpy change of the reaction under consideration, is then dependent on the net lattice energy differences of the two phases.

Discussion somewhat similar to the one delineated above have also been previously presented: In one case^{13} the hysteresis observed for the absorption–desorption of hydrogen on a palladium sponge was related to the phase changes of the metal from the α to the β phase. The exact nature of this change was not known and it is only mentioned that in the β phase, the metal hydride

(11) The arrangement of the molecules of the nonthermochromic phenyl derivative of **1** in the crystal lattice is very similar to that observed for **1b**.^{2}

(12) It is interesting to note that the lower phase transition observed for **1b** is hindered under pressure (cf. Figure 5). This is probably due to the arrangement of the substituents at the particular temperature (room temperature) that the pressure has been applied. At this temperature the substituents in each stack are positioned nearly directly opposing each other (cf. Figure 11). Application of pressure hinders the apparently necessary further shifting of them to allow intertwining and thus shrinkage of the cell in the *a* axis as the temperature is lowered.

(13) Everett, D. H.; Nordon, D. *Proc. R. Soc. London, Ser. A* **1960**, *A259*, 314.

was less dense. It can, however, be surmised that the volume increase in going from the α to the β phase is the result of an increase of the metal–metal bond length which is necessary to accommodate the metal hydride formed. Here again we can differentiate between two separate processes. One is the chemical reaction, i.e., the transformation of molecular hydrogen to atomic hydrogens chemically adsorbed on the metal atoms (hydride formation). The other is the lattice forces of the α phase resisting the expansion to the β phase. An indication of the correctness of this line of argumentation is the temperature dependence of the hysteresis loops observed[14] for the absorption–desorption of hydrogen on the LaNi$_5$ alloy. Thus, at higher temperatures, a higher pressure is required for loading (absorption) onto the alloy while the unloading (desorption) occurs at a relatively lower pressure. The result is an increase of the width of the hysteresis loop with rising temperature. As the metal–metal bonds tend to be somewhat longer at higher temperatures, hydrides once formed will tend to be more stable at that temperature, and only when the pressure is reduced well below the loading pressure isotherm, a spontaneous release of hydrogen concommitent with the return to the α phase is observed.

Another analysis of the forces underlying hysteresis is that forwarded for the pH- and (or) temperature-dependent hysteresis observed in the order–disorder reactions of solutions or colloids of polyelectrolytes such as certain polynucleotides.[15] The long-lived metastability in these biopolymers has, using the example of the dissociation–association of the three stranded model system poly A–2(poly U), been related to the interplay between the ionic interaction (H-bond formation and breakage) and the short-range field attractions between the polynucleotide chains. The latter force thus resemble the lattice forces in solids.

The proportional decrease of the width of the hysteresis loop with the decrease of the crystal size, observed for hydrogen adsorption on palladium metal and in the phase transformations of ammonium chloride[6] can also be related to the decrease of the lattice forces in very small crystallites.[16]

Finally, it should be pointed out that large hysteresis as found in the derivatives of **1** could in principle have a practical application. As the effect is not of a kinetic nature, the latent heat absorbed during the heating cycle is trapped and can be stored indefinitely as long as the temperature is not lowered below the lower transition temperature. Only after cooling below this temperature will the previously absorbed heat be spontaneously released. This forms in principle a heat storage battery. Unfortunately, the enthalpy changes observed for the various derivatives of **1** (cf. Table I) are insufficient for their efficient application for this purpose (cf. tables in ref 17).

Experimental Section

Differential scanning calorimetry (DSC) was generally carried out with a Du Pont 1090–910 calorimeter. Temperatures were typically scanned at 10 °C/min. The temperature scale was calibrated with pure indium (melting onset 156.63 °C) and with pure water (melting onset 0.0 °C) with an accuracy of ±0.15 °C. The energy coefficient was calibrated by the use of pure indium (heat of fusion 28.4 J/g) with an accuracy of 3%. Samples of 3–15 mg were weighed under argon and sealed in aluminum pans. The phase transition endo–exotherms were analyzed by computer, taking 150 data points/min. For the DSC measurements under pressure a SETARAM BT 215 calorimeter was used. About 250 mg of the sample was placed in special thick-walled cells of V 4A steel. Pressure was exerted by winding down a piston (lubricated screws) onto the sample. Pressure adjustments were achieved with a ratched wrench preset to the desired final torques of 20–80 (±0.5) N-m exerting pressures of roughly 0.5 to 2 kbar on the sample. After each scan and before changing the pressure to a new setting, the piston was unwound to release the previously applied pressure.

For the differential thermal analysis (DTA) an apparatus was used which allowed the observation of the sample during the temperature scans. Temperatures were measured by two iron constantan thermocouples inserted into the glass sample and the reference cells. These could be heated or cooled via a programmable thermostat. Scanning rates were typically 2.5 °C/min on about 30-mg samples.

Infrared investigations were carried out on a Nicolet 7199 FT-IR system. Samples were prepared as KBr pellets. For temperature regulation, a pellet holder equipped with a water jacket was used. Temperatures were measured with a small thermocouple inserted into the outer zone of the pellet. During the continuous heating and cooling cycles at an average rate of 2 °C/min, spectra were taken at 5 °C intervals. Each spectrum (average of 12 scans, 4-cm^{-1} resolution) was obtained in 9 s. The integrated absorbance of the 1760- and 1735-cm^{-1} bands which correspond to the hot modification were calculated by drawing base lines for each spectrum to minimize the interference by the neighboring peaks which also varied with temperature.

(14) Küppers, F. A.; van Mal, H. H. *J. Less-Common Met.* **1971**, *23*, 395.

(15) Neumann, E. *Angew. Chem.* **1973**, *85*, 430 *Angew Chem., Int. Ed. Engl.* **1973**, *12*, 356.

(16) For a further example and discussion on the effect of crystallite size on lattice forces, see: Yalpani, M.; Klotzbücher, W. E. *Z. Naturforsch., B*, in press.

(17) Fittipaldi, F. *Eur. At. Energy Community—EURATOM[Rep.]* **1981**, *EUR 6979*, 169.